ENVIRONMENTAL RESEARCH
LETTERS

LETTER • OPEN ACCESS

# Groundwater effects on net primary productivity and soil organic carbon: a global analysis

ENVIRONMENTAL RESEARCH
LETTERS

OPEN ACCESS

RECEIVED
17 December 2022

REVISED
4 June 2023

ACCEPTED FOR PUBLICATION
11 July 2023

PUBLISHED
27 July 2023



LETTER

# Groundwater effects on net primary productivity and soil organic carbon: a global analysis

**Bei Huang**[1,2], **Sam Zipper**[3], **Shaolin Peng**[1,*] and **Jiangxiao Qiu**[2,*]

[1] Sun Yat-sen University, School of Life Sciences, Guangzhou, People's Republic of China
[2] University of Florida, School of Forest, Fisheries, and Geomatics Sciences, Fort Lauderdale Research and Education Center, Davie, FL 33314, United States of America
[3] Kansas Geological Survey, University of Kansas, Lawrence, KS, United States of America
[*] Authors to whom any correspondence should be addressed.

**E-mail:** lsspsl@mail.sysu.edu.cn and qiuj@ufl.edu

**Keywords:** groundwater, ecosystem service, climate, land use, NPP, SOC, water table

Supplementary material for this article is available online

## Abstract

Groundwater affects ecosystem services (ES) by altering critical zone ecohydrological and biogeochemical processes. Previous research has demonstrated significant and nonlinear impacts of shallow groundwater on ES regionally, but it remains unclear how groundwater affects ES at the global scale and how such effects respond to environmental factors. Here, we investigated global patterns of groundwater relationships with two ES indicators—net primary productivity (NPP) and soil organic carbon (SOC)—and analyzed underlying factors that mediated groundwater influences. We quantitatively compared multiple high-resolution (~1 km) global datasets to characterize water table depth (WTD), NPP and SOC, and performed spatial simultaneous autoregressive modeling to test how selected predictors altered WTD-NPP and WTD-SOC relationships. Our results show widespread significant WTD-NPP correlations (61.5% of all basins globally) and WTD-SOC correlations (64.7% of basins globally). Negative WTD-NPP correlations, in which NPP decreased with rising groundwater, were more common than positive correlations (62.4% vs. 37.6%). However, positive WTD-SOC relationships, in which SOC increased with rising groundwater, were slightly more common (53.1%) than negative relationships (46.9%). Climate and land use (e.g., vegetation extent) were dominant factors mediating WTD-NPP and WTD-SOC relationships, whereas topography, soil type and irrigation were also significant factors yet with lesser effects. Climate also significantly constrained WTD-NPP and WTD-SOC relationships, suggesting stronger WTD-NPP and WTD-SOC relationships with increasing temperature. Our results highlight that the relationship of groundwater with ES such as NPP and SOC are spatially extensive at the global scale and are likely to be susceptible to ongoing and future climate and land-use changes.

## 1. Introduction

Groundwater is one of the most important freshwater resources, supporting agricultural, industrial and domestic water use (Siebert *et al* 2010, Gleeson *et al* 2020). However, accelerated withdrawal and depletion of groundwater, especially in arid and semi-arid regions (Aeschbach-Hertig and Gleeson 2012), challenges the long-term sustainability of freshwater resources (Wada *et al* 2012, de Graaf *et al* 2019, Elshall *et al* 2020). By altering ecohydrological and biogeochemical processes across the critical zone (i.e., a permeable layer of the Earth that extends from the top of the canopy to the bottom of weathered bedrock), changes in the water table depth (WTD) can cascade to affect a range of groundwater-dependent or -mediated ecosystem services (ES). Past work has revealed that groundwater impacts ES including biomass production, nutrient cycling, streamflow regulation and greenhouse gas mitigation (Danielopol *et al*

2000, Qiu *et al* 2019, Zipper *et al* 2022a). However, the spatial variations in the magnitude and direction of interactions between groundwater and ES at global scales remain poorly understood.

Primary productivity, as a fundamental indicator for many provisioning ES (e.g., crop and timber production), is sensitive to precipitation and limited by water availability (Churkina *et al* 1999, Wu *et al* 2011). In the sandy, humid forests of Wisconsin, USA, shallow groundwater (i.e., the near-surface portion of groundwater that can influence land surface processes) (Fan 2015, Hare *et al* 2021) increases tree growth by 63% compared to trees where groundwater was below the rooting depth (RD) (Ciruzzi and Loheide 2021). Nevertheless, groundwater effects on productivity are not always positive and vary in response to WTD and hydroclimatic conditions (Zipper *et al* 2015, Qiu *et al* 2019). In the cornfields of south-central Wisconsin, USA, both biophysical modeling and field experiments have revealed that shallow groundwater can subsidize crop water requirements and increase yield in dry years, while exerting a yield penalty in wet years by waterlogging and creating oxygen stress (Soylu *et al* 2014, Zipper *et al* 2015, 2017). A more recent global groundwater–vegetation analysis depicted complex positive or negative groundwater relationships with gross primary productivity (GPP), which were spatially heterogeneous and seasonally dynamic, and varied with vegetation type and regional climate (Koirala *et al* 2017). However, global-scale patterns of groundwater effects on net primary productivity (NPP) remain unclear and may differ from GPP because (1) soil evaporation and plant transpiration are highly responsive to soil moisture that is susceptible to groundwater influences (Maxwell and Condon 2016) but not reflected in GPP; and (2) the ratio of NPP to GPP is not always constant spatially (Collalti and Prentice 2019) or temporally. Thus, we may expect that groundwater effects on NPP may show a different pattern from WTD-GPP covariation as previously revealed across the globe.

Groundwater also significantly affects regulating ES; for example, by influencing climate regulation through changes in soil carbon storage (Qiu *et al* 2019). Many regional studies (e.g., in coastal wetlands and riparian zones) have found that WTD was positively correlated with soil organic carbon (SOC) (Lyon *et al* 2011, Guan *et al* 2021), indicating greater SOC content with rising groundwater. In tropical peatlands, mainly located in Southeast Asia, soil $CO_2$ emissions can be amplified (i.e., leading to reduced SOC) with increases in WTD due to enhanced soil respiration and decomposition (Prananto *et al* 2020). NPP also provides a net carbon input into ecosystems (Chapin *et al* 2011), suggesting that positive groundwater effects on NPP could lead to more organic carbon input into soils. However, rising groundwater levels do not always improve SOC stocks and $CO_2$ emissions are not consistently dependent on WTD (Tiemeyer *et al* 2016). The net effects of groundwater on SOC, especially at continental and global scales, remain elusive and can be highly variable depending on complex interactions between WTD, WTD-mediated soil abiotic and biotic conditions, C inputs and outputs, and climatic conditions (Meersmans *et al* 2011, Chen *et al* 2022).

In tandem, groundwater effects on ES can be positive or negative, highly variable spatially, and likely differ by ES and mediated by environmental factors (Qiu *et al* 2019, Wen *et al* 2020). In a global climate change context, multiple environmental factors could interact to alter the dynamics of groundwater as well as its long-term impacts on ES, including climate (Cuthbert *et al* 2019), soil texture (Qiu *et al* 2019, Huang *et al* 2021) and topographic factors such as slope and elevation (Fan *et al* 2013, Maxwell and Condon 2016). Yet the global interplay between these potential drivers of WTD-ES relationships has not been thoroughly investigated. Hence, in this paper, we ask two main questions: (1) how does groundwater relate to NPP and SOC at the global scale? and (2) how do environmental factors (i.e., climate, topography, soil and land use/cover) mediate groundwater depth's relationships with NPP and SOC? To answer these questions, we first developed a transferrable analytical framework to quantify the relationship between ES and groundwater availability (indicated by WTD) (figures 1(a) and (b)), which can be further mediated by environmental factors at the global scale (figure 1(c)). We then empirically investigated these relationships by quantitatively comparing high-resolution global datasets of WTD and two ES indicators (NPP and SOC) and an array of selected environmental covariates.

## 2. Methods

### 2.1. Data sources and preprocessing

Our overall analytical procedure is shown in the flowchart (figure S1) and details of data sources are shown in table 1. The WTD dataset and the RD dataset were obtained from steady-state global model simulations (Fan *et al* 2013, 2017; figures S2 and S3). The long-term NPP datasets were derived from the global annual products of Collection 5.5 MOD17A3, from the Numerical Terradynamic Simulation Group, University of Montana. To match the long-term average WTD dataset, we estimated long-term average global NPP as the mean from 16 years (2000–2015) of available NPP data for subsequent analyses (figure S4). SOC stock datasets were obtained from the SoilGrids250m (Hengl *et al* 2017). We calculated SOC for one shallow soil layer from 0 to 15 cm depth (i.e., $SOC_{[0–15\,cm]} = SOC_{[0–5\,cm]} + SOC_{[5–15\,cm]}$), representative of the most active soil layer (Jobbágy and Jackson 2000, Deng *et al* 2014),

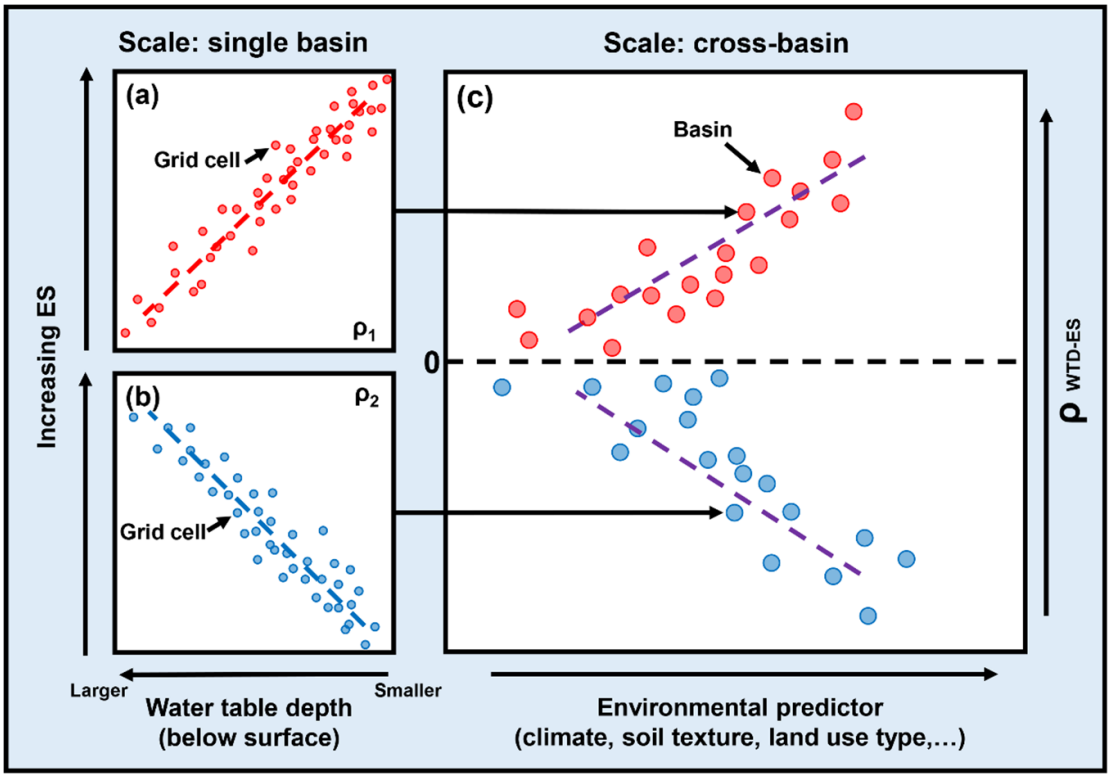


**Figure 1.** Conceptual framework illustrating hypothesized groundwater effects on ES and how external environmental factors could mediate groundwater effects at the basin scale across the globe. In this study, the specific two ES indicators investigated are NPP and SOC. (a) Illustrated hypothetical positive WTD-ES correlations at basin scale; (b) illustrated hypothetical negative WTD-ES correlations at basin scale. In panels (a) and (b), red and blue points represent WTD and ES values for all the grid cells within a basin, and the dash lines indicate the fitted WTD-ES relationships. As a result, each basin has a single correlation coefficient ($\rho$) to denote the magnitude and direction of groundwater effects. (c) Scatter plots showing how WTD-ES coefficients (i.e., $y$-axis) respond to environmental factors (i.e., $x$-axis). In panel (c), each point represents basin-level estimated $\rho_{\text{WTD-ES}}$ values and the fitted dash line indicates predictor–coefficient correlation across all basins of the globe.

**Table 1.** Summary of global datasets used this study.

| Variable | Unit | Temporal resolution | Spatial resolution | Source |
|---|---|---|---|---|
| WTD | Meters below land surface | Static | 30 arcsec (∼1 km) | Mechanistic model, calibrated by 1.6 million site observations (Fan *et al* 2013) |
| RD | Meters below land surface | Static | 30 arcsec (∼1 km) | Mechanistic model, exhibiting the same behavior as 2200 site observations (Fan *et al* 2017) |
| NPP | Kg C $m^2$ | Annual average (2000–2015) | 1 km | Satellite product from Numerical Terradynamic Simulation Group (http://files.ntsg.umt.edu/data/NTSG_Products/MOD17/GeoTIFF/MOD17A3/) |
| SOC stock | t/ha | Static | 0.25 km | Global observation-based model (https://files.isric.org/soilgrids/latest/data/; Hengl *et al* 2017) |
| Basin boundary and environmental factors | Details see table 2 | Static | 15 arcsec (∼500 m) | A standardized compendium of hydro-environmental information, the HydroBASINS database (level 07 basins) (www.hydrosheds.org/hydroatlas; Linke *et al* 2019) |

and another deep soil layer from 0 to 200 depth (i.e., $SOC_{[0–200\ cm]} = SOC_{[0–5\ cm]} + SOC_{[5–15\ cm]} + SOC_{[15–30\ cm]} + SOC_{[30–60\ cm]} + SOC_{[60–100\ cm]} + SOC_{[100–200\ cm]}$), indicative of the total soil carbon pools (figure S5). All these global datasets were from independent sources quantified with different approaches and/or estimated using different variables, thus avoiding any potential circularity in the analyses.

While these datasets represented the best-available global products, there were some inherent challenges linking and analyzing them together. First, the underlying data used to generate these globally gridded products were spatially heterogeneous, with a bias towards more measurements and representation in temperate North America and Europe and fewer in Africa, Asia and high latitudes, which could cause inconsistent accuracy of WTD, NPP and SOC datasets. Second, these datasets were from multiple sources with different temporal coverages, making it impossible to match them temporally under a same time period. For example, the WTD and SOC datasets lumped together observations from many years to create a single static dataset, while mean annual NPPs were calculated by averaging all the annual estimates from 2000 to 2015. Given the spatial heterogeneity and temporal asynchrony of datasets, our study aims to depict the fundamental patterns of WTD-NPP and WTD-SOC relationships with typical data that reflected long-term natural conditions, rather than an analysis of inter- or intra-year dynamics.

All datasets were adjusted to a consistent spatial resolution of 30 arcsec (~1 km). To filter out grid cells that were not expected to be influenced by groundwater, we calculated the gap distance between expected water table and RDs, since prior research has revealed that groundwater exerted the most profound impacts in shallow groundwater environments, but produced negligible influences in deep groundwater areas (Orellana *et al* 2012, Fan *et al* 2013, Qiu *et al* 2019). Here, we restrict our analysis to areas where the gap distance was $\leqslant$5 m as a conservative threshold (more details in the supplementary information (SI)).

### 2.2. Spatial scale of analysis

The WTD-NPP and WTD-SOC relationships were estimated at the basin scale, as defined using level 07 of the HydroBASINS dataset (figure S6) (Linke *et al* 2019). We used HydroBASINS since it was derived from the same digital elevation model as the WTD dataset (Fan *et al* 2013). Basins with areas <100 $km^2$ or with <30 grid cells of WTD-NPP or WTD-SOC data were filtered out to avoid unrobust results (see the SI for details). After this screening, the final WTD-NPP dataset included 45 963 basins with an average basin size of 2581.3 $km^2$ and the final WTD-SOC dataset included 50 001 basins with an average basin size of 2585.2 $km^2$.

### 2.3. Estimating WTD-NPP and WTD-SOC relationships

To address our first question, Spearman's correlation coefficient, $\rho_{(x-y)}$, was calculated to quantify the basin-scale relationships between $WTD_{(x)}$ and $NPP/SOC_{(y)}$ across the globe. Spearman's correlation is robust to data distribution and has been previously used to estimate WTD-NPP and WTD-SOC relationships (Mitchell *et al* 2014, Koirala *et al* 2017). When calculating $\rho_{(x\_y)}$, the WTD value was transformed into a negative value (-WTD) so that interpretation of the ecohydrological implications of WTD-NPP and WTD-SOC correlations was more intuitive. Specifically, this meant that basins with $\rho > 0$ had greater NPP or SOC when the water table was closer to the land surface (i.e., positive NPP/SOC response to shallow groundwater, as depicted in figure 1(a)), and basins with $\rho < 0$ had greater NPP or SOC when the water table was deeper from the land surface (i.e., negative NPP/SOC response to shallow groundwater, as depicted figure 1(b)). We analyzed the distributions of Spearman's correlation, $\rho_{(x-y)}$, within 20°-latitude bins and across eight geographic regions as defined based on continents from HydroBASINS (excluding Greenland and Antarctica). As noted above, the confidence of estimated $\rho_{(x-y)}$ for each bin or geographic region was subject to confidence in the underlying data. Varying densities of WTD observations were used to generate the global WTD input dataset (see details in section S5 of the SI). Specifically, the confidence of simulated WTD data in North America, Australia and Europe could be higher than the confidence in Asia or Africa (table S1), indicating that the confidence of our derived WTD-NPP/SOC correlations may be similarly higher in North America, Australia and Europe than in other regions. In addition, the terrain and landscape factors affected the confidence of the simulated global WTD dataset (Fan *et al* 2013), and thus the confidence of our WTD-NPP/SOC correlations may be greater in areas with flatter topography or with more natural vegetation (see the SI for more details).

### 2.4. Analyzing effects of environmental factors on WTD-NPP and WTD-SOC relationships

In addressing our second question, to avoid mixing correlations with potentially different mechanistic reasons, we first separated all basins into positive and negative subsets based on the sign of their WTD- NPP and WTD-SOC correlations. We then extracted from HydroATLAS (Linke *et al* 2019) a total of 13 environmental factors that were hypothesized to mediate groundwater influences on NPP and SOC (table 2). All environmental factors were standardized before statistical modeling and their correlation matrix was constructed to identify and filter out highly collinear factors.

**Table 2.** Summary of potential environmental factors extracted from HydroATLAS (Linke *et al* 2019).

| Environmental factors | Period | Dimension | Value range | Unit | Source data | References |
|---|---|---|---|---|---|---|
| Elevation | 2000–2010 | Average | −86–5800 | Metres a.s.l. | EarthEnv-DEM90 | Robinson *et al* (2014) |
| Terrain slope | 2000–2010 | Average | 0–34.5 | Degrees | EarthEnv-DEM90 | Robinson *et al* (2014) |
| Air temperature | 1950–2000 | Annual average | −23.8–31.2 | Degrees celsius | WorldClim v1.4 | Hijmans *et al* (2005) |
| Precipitation | 1950–2000 | Annual average | 0–7391 | Millimetres | WorldClim v1.4 | Hijmans *et al* (2005) |
| Global aridity index | 1960–1990 | Average | 0–11.46 | Unitless | Global Aridity Index | Zomer *et al* (2008) |
| Irrigated area extent (equipped) | 1900–2005 | Spatial extent | 0–99 | Percent cover | HID v1.0 | Siebert *et al* (2015) |
| Clay fraction in soil | | Average | 2–43 | Percent | SoilGrids1km | Hengl *et al* (2014) |
| Silt fraction in soil | | Average | 2–60 | Percent | SoilGrids1km | Hengl *et al* (2014) |
| Soil erosion | | Average | 0–98 935 | kg/hectare per year | GloSEM v1.2 | Borrelli *et al* (2017) |
| Urban extent | 2015 | Spatial extent | 0–100 | Percent cover | GHS S-MOD v1.0 (2016) | Pesaresi and Freire (2016) |
| Natural vegetation extent | 2000 | Spatial extent by class | 0–100 | Percent cover | GLC2000 | Bartholomé and Belward (2005) |
| Semi-natural vegetation extent | 2000 | Spatial extent by class | 0–100 | Percent cover | GLC2000 | Bartholomé and Belward (2005) |
| Cultivated area extent | 2000 | Spatial extent by class | 0–100 | Percent cover | GLC2000 | Bartholomé and Belward (2005) |

We then built a fully linear model and used *Moran's I* to test for potential spatial autocorrelation. Since our analyses revealed significant spatial autocorrelations in residuals, we used the spatial simultaneous autoregressive (SAR) model for spatial regression, which was conducted with the spatial dependence (i.e., spdep) package in R (Bivand 2022). Depending on the volume of datasets and number of predictors, we either used the 'dredge' function in the Multi-Model Inference (i.e., MuMIn) package in R (Barton 2009) or a consistent model selection process (see the SI for details) to determine the optimal SAR model for each dataset that had the lowest Akaike's information criteria values (Burnham and Anderson 2004).

Based on the results of optimal SAR models, we then used scatterplots to visualize the responses of WTD-NPP and WTD-SOC correlations to the strongest mediating environmental factors. Since the responses could be highly scattered, we used the constraint line analysis to characterize the response curves (Cade and Noon 2003, Qiao *et al* 2019, Liu and Wu 2021). Specifically, adopted from Mills *et al* (2006), the segmented quantile regression method was used to generate response curves for the upper and lower boundaries of each scatter plot to characterize and visualize how environmental factors affected the strongest WTD-NPP or WTD-SOC relationships (see the SI for details). All the analyses were conducted in R 4.2.1 (R Core Team 2022).

## 3. Results

### 3.1. Global distribution of WTD-NPP and WTD-SOC relationships

Globally, 61.5% of all basins showed significant correlations between simulated WTD and long-term mean NPP, with Spearman's correlation coefficients ranging from −0.94 to 0.83. There were more basins with negative WTD-NPP correlations than positive correlations (62.4% vs. 37.6%, respectively, out of basins with significant correlations; figure 2(a)). Negative WTD-NPP correlations (indicating decreased NPP at shallower WTD) were primarily located in high northern latitudes and aggregated

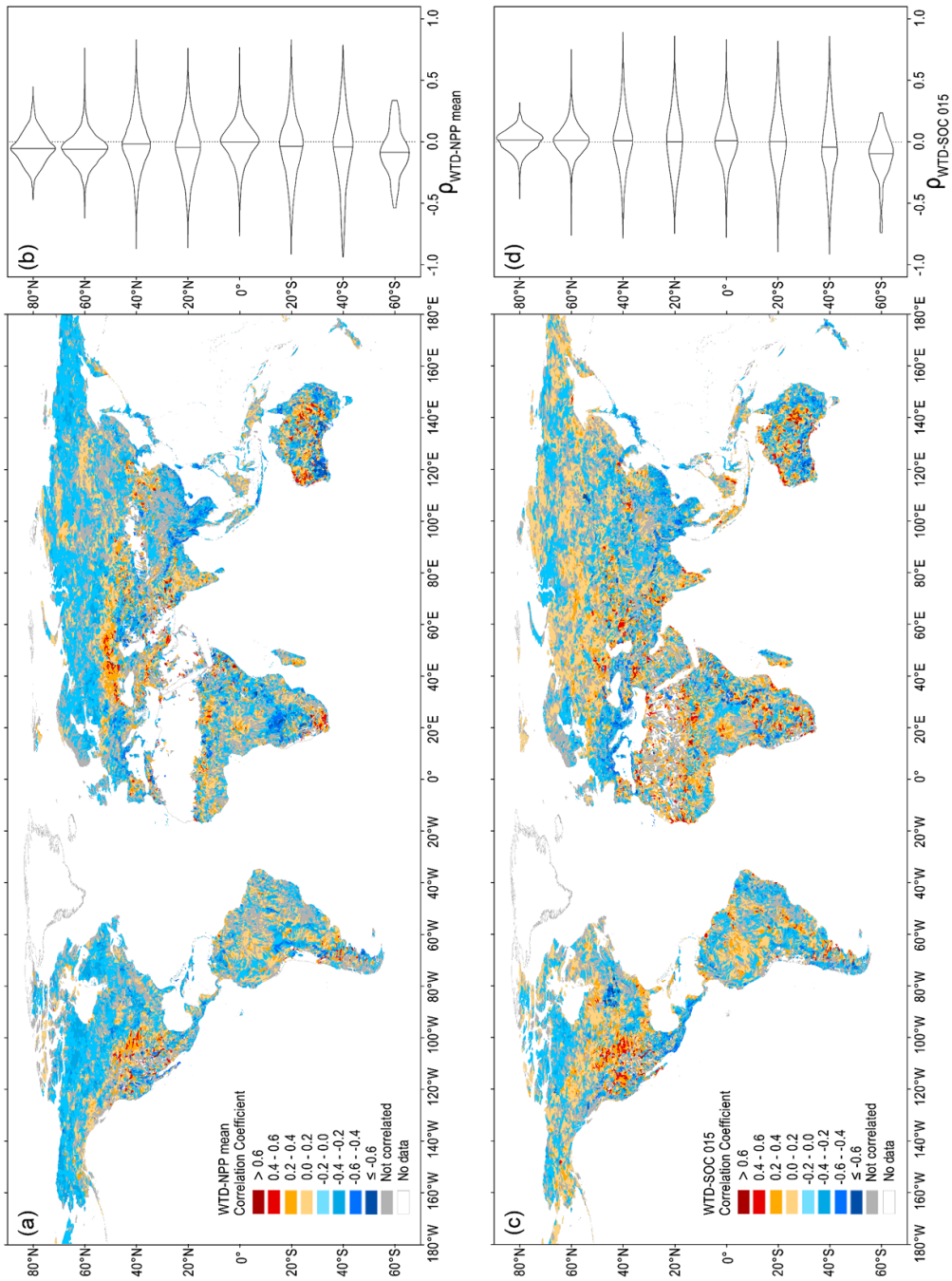


**Figure 2.** (a) Global pattern of WTD correlations with annual average NPP (2000–2015); (b) distribution of correlation coefficient of WTD-NPP mean at latitude intervals of 20°; (c) global pattern of WTD correlations with SOC at 0–15 cm depth from land surface (SOC 015); (d) distribution of correlation coefficient of WTD-SOC relationships (i.e., 0–15 cm soil depth from land surface) at latitude intervals of 20°. WTD-SOC 015: WTD- SOC relationships at 0–15 cm soil depth. The color gradient from red to blue indicates the sign and magnitude of the Spearman's correlation and the white color indicates regions with no available data.

clusters in southern Asia, mid-southern Africa and southern Australia. Positive WTD-NPP correlations (indicating increased NPP at shallower WTD) were mainly found in Central Europe, mid-western North America, western and central Australia, and Southern Africa. Median values and ranges of Spearman's correlation coefficients, $\rho_{(\text{WTD-NPP mean})}$, slightly decreased from the equator to the poles, with a similar unimodal distribution for each latitude group, but the distribution of $\rho_{(\text{WTD-NPP mean})}$ in high latitudes showed overall smaller ranges (figure 2(b)). The global pattern of WTD-NPP standard deviation correlations and distribution of $\rho_{(\text{WTD-NPP standard deviation})}$ were broadly similar to those of WTD-NPP mean correlations, though certain hotpots of positive or negative correlations varied slightly (figure S7).

For SOC, 64.7% of all basins showed significant correlations between WTD and SOC at the 0–15 cm depth, of which 53.1% were positive and 46.9% negative (figure 2(c)). The positive WTD-SOC correlations (indicating increased SOC with shallower WTD) were most common in arid or seasonally dry regions with diverse geography, such as mid-northern Europe, southern India and mid-western North America, and especially strong in the desert and steppe of Africa and Australia (figures 2(c) and 3(b)). Basins with negative WTD-SOC correlations (indicating decreased SOC with shallower WTD) were mainly located in mid-eastern and southern North America and southeastern Asia. The distributions of Spearman's correlation coefficients, $\rho_{(\text{WTD-SOC 015})}$ were symmetric with long tails within each 20°-latitude bin, except for 70°–90° North and 50°–70° South (figure 2(d)). Median values of the correlation coefficients were generally around zero but decreased at lower latitudes in the Southern Hemisphere. Hotspots of WTD-SOC correlations in the deep soil layer (i.e., 0–200 cm) and distribution patterns of $\rho_{(\text{WTD-SOC 0200})}$ were similar to the results of WTD-SOC relationships at the 0–15 cm depth (SI section S9). However, there were more positive WTD-SOC relationships at the 0–200 cm soil depth, where 70.6% of all basins with significant WTD-SOC correlations showed positive relationships at the global scale (figure S7).

At regional to continental scales, most correlation coefficient distributions were symmetric with long tails spanning nearly the full −1.0–+1.0 range, though distributions for the Arctic and Siberia have smaller ranges than in other regions (figures 3 and S8). However, as noted previously, empirical training and validation data for WTD, SOC and NPP datasets were more limited in these regions, which may affect accuracy and reduce confidence in our findings for these geographic settings. For WTD-NPP correlations, coefficient medians of different regions were consistently negative, aligning with the result that negatively correlated basins were more common across the globe (figure 3(a)). However, medians of WTD-SOC correlation coefficients were essentially zero except for Africa, which was slightly positive (figure 3(b)).

### 3.2. Environmental factors mediating WTD-NPP and WTD-SOC relationships

Across the subset of basins with positive or negative WTD-NPP and WTD-SOC relationships, the optimal SAR models showed pseudo $R^2$ values ranging from 0.19 to 0.29 (table S3). The pseudo $R^2$ values ranged from 0.21 to 0.29 for WTD-NPP mean and WTD-SOC (at 0–15 cm depth) relationships (figure 4), while pseudo $R^2$ values ranged from 0.19 to 0.29 for WTD-NPP standard deviation and WTD-SOC (at 0–200 cm depth) relationships (figure S10). Overall, climate factors were the dominant predictors for WTD-NPP and WTD-SOC relationships at the basin scale across the globe. By comparing all predictors in each optimal SAR model, the annual average air temperature showed the strongest influence on mediating WTD-NPP/SOC relationships (figures 4 and S10). Specifically, the strength of positive correlations between WTD vs. NPP and SOC responded positively to temperature, indicating that at higher temperatures, greater NPP and SOC were associated with shallower WTD. On the other hand, for basins with negative WTD-NPP and WTD-SOC relationships, the strength of negative correlations responded negatively to temperature, meaning that at higher temperatures, NPP and SOC were more strongly negatively related with WTD.

Segmented quantile regressions showed that optimal constraint lines (i.e., those with the highest $R^2$) were quadratic for both NPP and SOC. Constraint effects of the annual average air temperature on the potential maximum of positive WTD-NPP/SOC correlations (i.e., points on the upper constraint lines) first increased and then flattened (figures 5(a), (d) and S11(a), (d)). Temperature constraint effects were symmetric for positive and negative WTD-NPP/SOC correlations, and the potential minimum negative WTD-NPP and WTD-SOC coefficients (i.e., points on the lower constraint lines) first decrease and then flattened with rising temperature. Collectively, these results showed that higher temperatures tended to either boost positive effects of groundwater or amplify negative groundwater influences.

Most optimal SAR models for NPP and SOC also contained annual average precipitation as a significant predictor. Precipitation was generally a weaker predictor and showed opposite effects from temperature; for instance, positive WTD-NPP/SOC relationships decreased in magnitude as precipitation increases (figures 4 and S10). Such relationships were consistent with the effects of the global aridity index on WTD-NPP and WTD-SOC correlations (figures 4 and S10), with data points more clustered in the

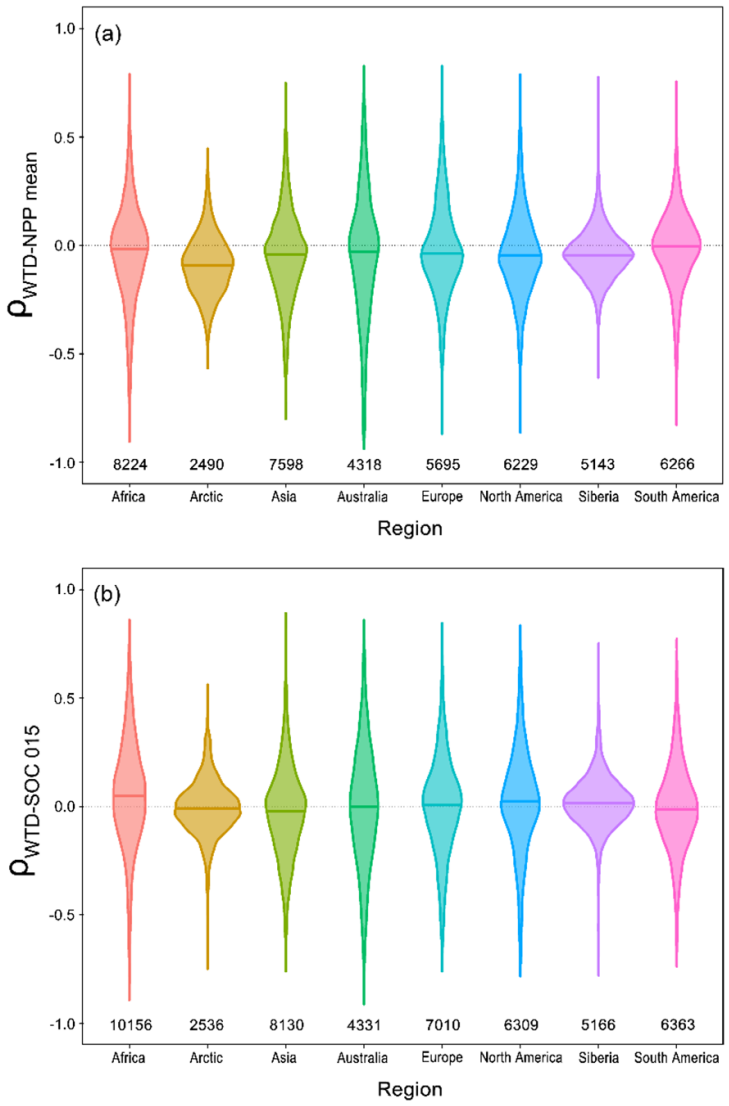


**Figure 3.** Distribution of correlation coefficients of (a) WTD-NPP mean and (b) WTD-SOC 015 across different continental regions. WTD-SOC 015: WTD-SOC relationships at 0–15 cm soil depth. The number at the bottom of each violin plot represents the number of basins included in the analysis for each continental region.

lower range of the global aridity index (figures 5(c), (f) and S11(c), (f)). Segmented quantile regressions showed that the potential maximum of positive WTD-NPP/SOC correlations decreased, and potential minimum of negative WTD-NPP/SOC correlations increased with rising precipitation (figures 5(b), (e) and S11(b), (e)). Collectively, these results showed that stronger precipitation or greater humidity both weakened positive and negative groundwater effects on NPP and SOC.

The correlations with land use differed between WTD-NPP and WTD-SOC, and mainly reflected vegetation extent including natural, semi-natural vegetation and cultivated area (figures 4 and S10). Specifically, the magnitude of positive WTD-NPP correlations was negatively correlated with natural vegetation extent, indicating that potential increases in NPP associated with shallower WTD were lower in settings with more natural vegetation cover. Meanwhile, the magnitude of negative WTD-NPP correlations were positively correlated with natural, semi-natural and cultivated area extent, meaning that negative WTD-NPP relationships were weaker in settings with increasing extent of these cover types. Consistently, both results suggested that groundwater relationships with NPP were weaker in basins with higher vegetation extent. In contrast, models of WTD-SOC correlations contained fewer land use factors with smaller effects. Overall, our results showed that increasing vegetation extent had the potential to enhance positive groundwater effects, while weakening negative groundwater effects on SOC. Topographic factors, irrigated area extent, soil erosion, and soil texture were not retained in the final optimal SAR models, with weak to negligible relationships across all candidate models.

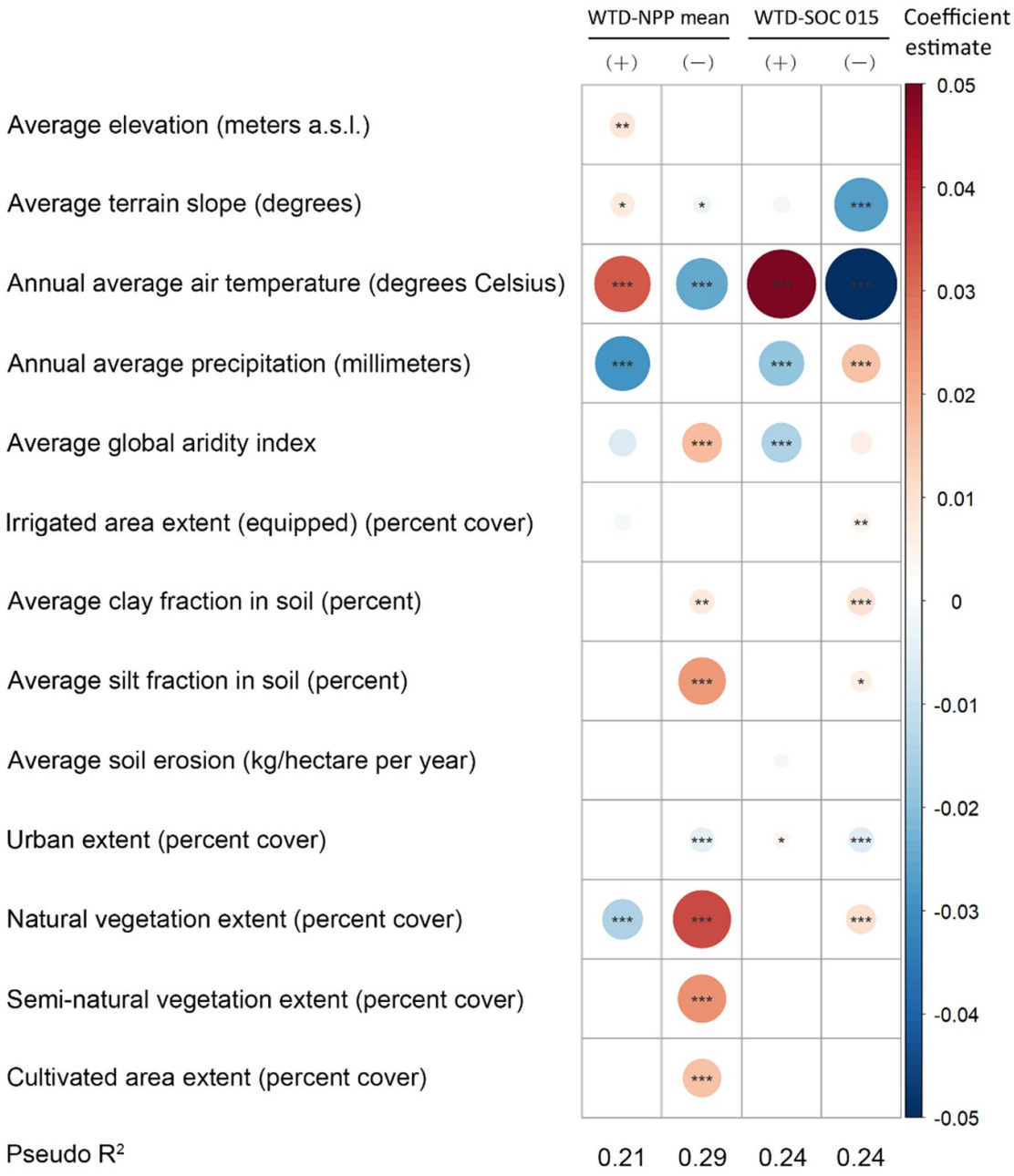


**Figure 4.** Results of the optimal spatial SAR models. WTD-NPP mean: the optimal SAR models for the effects of environmental factors on relationships between WTD and annual averaged NPP; WTD-SOC 015: the optimal SAR models for the effects of environmental factors on WTD-SOC relationships at 0–15 cm depth. Sign '(+)' represents results from analysis of a subset of basins with positive WTD-NPP/SOC relationships and '(−)' represents the results from the subset of negative WTD-NPP/SOC relationships. Positive correlations are displayed in red and negative correlations in blue. The color intensity and the size of the circles are proportional to correlation coefficients. The *p*-value of significant coefficient was shown as: *p*-value $< 0.001$: ***, $<0.01$: **, $<0.05$: *. Blank cells mean the predictor was not retained in the SAR model from model selection.

## 4. Discussion

### 4.1. Global pattern of WTD-NPP and WTD-SOC relationships

Groundwater depth variation was significantly correlated with NPP and SOC at the basin scale across the globe, indicating a strong groundwater influence on these ES indicators. However, WTD-NPP and WTD-SOC correlations were spatially heterogeneous and differed between NPP and SOC, indicating that groundwater effects on NPP and SOC are highly context-specific and mediated by environmental factors such as climate or ecohydrological conditions. For instance, WTD can affect plant transpiration and soil evaporation (Maxwell and Condon 2016), which could lead to effects on plant growth by modifying root water availability (Soylu *et al* 2014). Similar to global WTD-GPP correlations revealed in Koirala *et al* (2017), we found that positive WTD-NPP correlations were dominant in arid and semi-arid regions (e.g., the Great Plains of North America, the Eurasian Pontic–Caspian steppe; figure 2(a)),

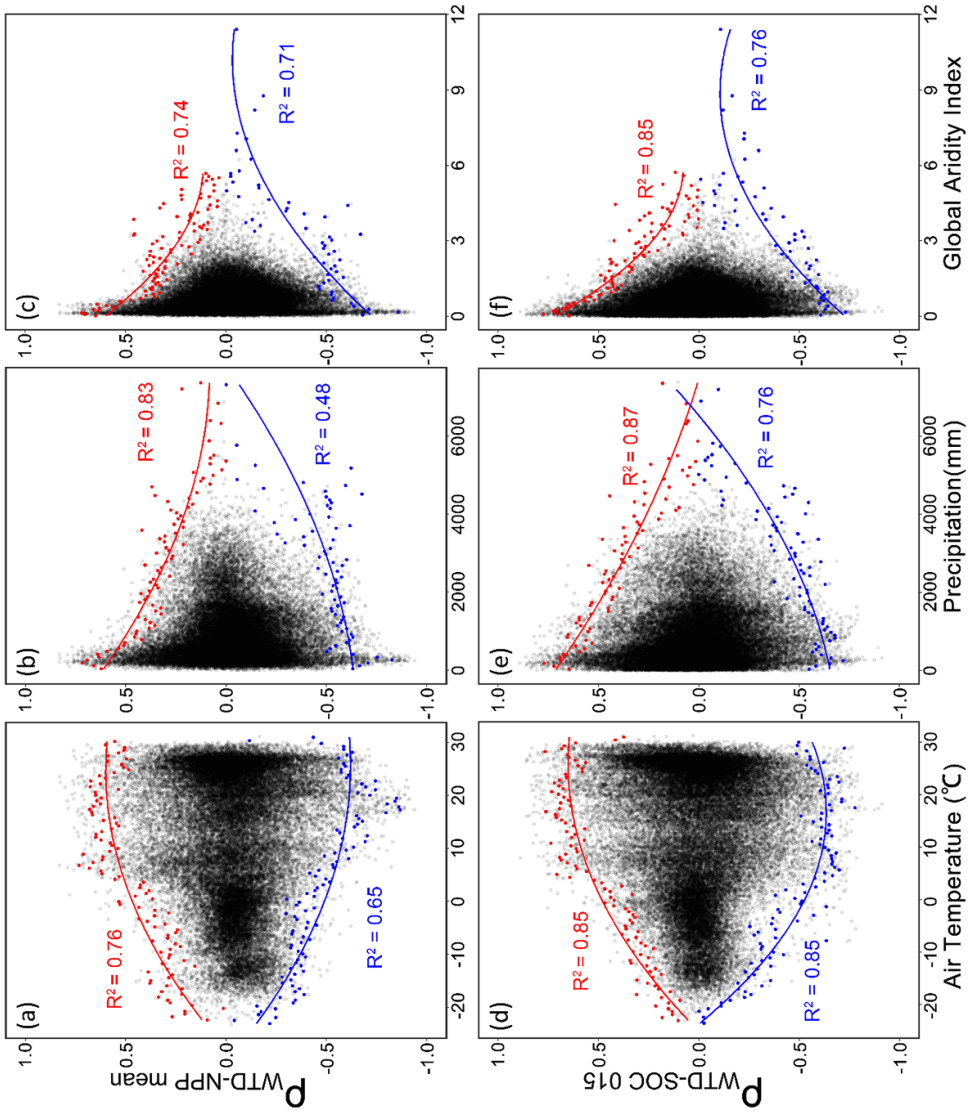


**Figure 5.** Responses of WTD-NPP and WTD-SOC correlations to different climate factors. (a) Responses of WTD-NPP mean correlation to annual average air temperature; (b) responses of WTD-NPP mean correlation to annual average precipitation;
(c) responses of WTD-NPP mean correlation to average global aridity index; (d) responses of WTD-SOC 015 correlation to annual average air temperature; (e) responses of WTD-SOC 015 correlation to annual average precipitation; (f) responses of WTD-SOC 015 correlation to average global aridity index. WTD-SOC 015: WTD-SOC relationships at 0–15 cm soil depth. Blue points are 1% quantiles of datasets and red points are 99% quantiles of datasets. Blue and red lines are 1% and 99% quantile regression lines, respectively.

where shallow groundwater can provide a water subsidy for enhancing productivity during dry periods (Zipper *et al* 2015, Rizzo *et al* 2018). In contrast, more negative WTD-NPP correlations were distributed in humid and water abundant regions (e.g., South Asia, northern Eurasia, figure 2(a)), where increasing WTD could lead to oxygen stress from waterlogging that, in turn, negatively affects NPP (Wen *et al* 2020).

While we generally observed similar WTD-NPP patterns to the WTD-GPP relationships found in Koirala *et al* (2017), there are key distinctions between WTD, NPP and GPP datasets used in our work as well as our processing workflows for analyzing WTD-ES relationships. To complement our WTD-NPP analysis and better compare findings from Koirala *et al* (2017), we conducted an additional global analysis on WTD-GPP relationships using our datasets and workflow (details and full results in section S10 in SI). Essentially, when comparing WTD-NPP (figure 2) and WTD-GPP (figure S9) patterns in our study, we found primarily similar patterns globally but some minor regional differences. For example, in eastern North America, WTD-NPP relationships were mostly negative, while WTD-GPP relations were mostly positive. Differences between WTD-NPP and WTD-GPP relationships may be due to large-scale spatial variability of NPP:GPP ratios (Zhang *et al* 2009). This work found that NPP:GPP ratios were low (from 0.45 to 0.6) in eastern Northern America, which could cause differences in the WTD-NPP and WTD-GPP correlations in this region. The strong WTD-NPP and WTD-GPP coupling as we observed at the global scale suggests that shallow groundwater may be a critical explanatory factor for spatial heterogeneity of NPP:GPP ratios by changing shallow soil moisture that influences autotrophic respiration and $CO_2$ fluxes (Green *et al* 2019). However, more work would be needed to investigate the strength of such interactions at the global scale.

Comparing our WTD-GPP patterns with those in Koirala *et al* (2017), we also found spatially similar patterns with some notable regional differences. For example, we found more basins with significant WTD-GPP correlations (either positive or negative) in our analysis, especially in the middle of North America and some parts of southern Asia (figure S9). These results suggest that the higher-resolution gridded GPP datasets we used (∼1 km resolution, compared to ∼10 km from Koirala *et al* 2017) can capture fine-scale ecosystem responses to WTD that can be masked in coarser resolution analyses. Further, Koirala *et al* (2017) did not investigate groundwater effects on GPP above 60°N, where we observed widespread negative WTD-NPP and WTD-GPP relationships in perennial cold and humid tundra regions at high Northern Hemisphere latitudes (figures 2(a) and (b)), though this finding needs to be cautiously interpreted due to the underrepresentation of empirical observations for developing the WTD and NPP datasets for these high latitude regions. These results suggest potential negative relationships between excessive water availability caused by shallow groundwater and plant productivity extend outside of temperate environments where most research on the topic has occurred (Liu *et al* 2020). Overall, our work complements and expands on the important past findings of Koirala *et al* (2017).

As an important predictor of SOC, groundwater can significantly affect greenhouse gas fluxes (Turetsky *et al* 2014) and influence the dynamics and spatial variations in SOC. Our results revealed more basins with positive WTD-SOC relationships at the global scale, both for the most active soil layer (0–15 cm, figure 2(c)) and deeper SOC pools (0–200 cm, figure S7(c)). Such positive WTD-SOC correlations were most common in arid or seasonally dry regions with diverse geography, especially in the desert and steppe areas in Africa (figures 2(c) and 3(b)). Based on the dynamics observed in regional studies (Lyon *et al* 2011, Guan *et al* 2021), the underlying mechanism for positive WTD-SOC may be that when WTD is shallower, pore space oxygen deficiency due to increased soil moisture inhibits decomposition of organic matter, which causes SOC accumulation (Callesen *et al* 2003). Moreover, groundwater could regulate carbon exchange indirectly by regulating nitrogen availability in the plant–soil system and a shallower WTD may enhance $CO_2$ inputs from GPP over $CO_2$ emissions by ecosystem respiration, ultimately affecting SOC (Pohl *et al* 2015). Variations in deep groundwater can still impact SOC in the top soil layer (Poeplau *et al* 2020), through regulating heterotrophic respiration (i.e., non-plant root respiration, Prananto *et al* 2020). However, WTD effects on different soil gas fluxes in previous studies have been inconsistent and nonlinear (Pohl *et al* 2015), or not even correlated (Tiemeyer *et al* 2016). For example, in seasonally well-drained wetlands without perennial frozen soil at high latitudes, an elevated WTD potentially promoted soil $CH_4$ emissions and thus reduced SOC (Turetsky *et al* 2014), which may explain negative WTD-SOC correlations in some high-latitude Northern Hemisphere basins (figure 2(c)).

### 4.2. Environmental factors mediating WTD-NPP and WTD-SOC relationships

Optimal SAR regression models demonstrated that multiple environmental factors could mediate WTD-NPP and WTD-SOC correlations, of which climate and land use were the most notable factors (figures 4, S10 and table S3).

Specifically, climate effects had a similar mediating role for both WTD-NPP and WTD-SOC relationships (figures 4 and S10). For basins with an annual average air temperature >16 °C (thresholds of constraint effects were shown in table S4), a shallower

WTD either promoted positive groundwater effects on ES or amplified negative effects. These results suggested that rising water tables subsidize crop production by enhancing root water uptake to promote NPP or SOC in warmer regions (Lowry and Loheide 2010, Jobbágy *et al* 2011), while in cooler settings shallow groundwater introduced anaerobic effects to reduce evapotranspiration, NPP and reduced SOC accumulation (Soylu *et al* 2014). In contrast, for basins with higher annual average precipitation (or higher humidity), both positive and negative WTD-NPP/SOC correlations were weakened. Since vegetation prefers to obtain water from the soil water caused by recent precipitation infiltration or past infiltration stored in deep soil (Miguez-Macho and Fan 2021), increasing precipitation and air moisture may diminish the relative importance of groundwater, but the extent of diminishment of groundwater may differ among climate zones. It is noteworthy that under high-temperature conditions, quadratic constraint regression lines turned from upward to flat (figures 5(a), (d) and S11(a), (d)), indicating that potential maximum groundwater effects on NPP and SOC were limited and groundwater's influences on NPP and SOC may be lessened in future warmer climate conditions.

In contrast to climate, the effects of land use on WTD-NPP and WTD-SOC relationships were different between NPP and SOC, with mediating effects from four types of land use extent (figure 4). Weaker positive and negative WTD-NPP correlations were associated with higher vegetation extent in basins. Hence, vegetation extent showed similar mediating effects on WTD-NPP relationships as precipitation, potentially indicating that the extent of vegetation, especially natural vegetation, may weaken groundwater effects on NPP through increasing forest rainfall (Staal *et al* 2018) or enhancing rainfall interception (Porada *et al* 2018). For WTD-SOC correlations, greater vegetation extent appeared to promote positive groundwater effects in basins with a positive WTD-SOC correlation, while weakening negative groundwater effects in basins with a negative WTD-SOC correlation. Similarly, the normalized vegetation index has been proven to have a strong positive correlation with SOC (Bangroo *et al* 2020), indicating that vegetation extent should be highly positively correlated with SOC.

### 4.3. Implications for groundwater management and research limitations

Our study revealed widespread basin-scale relationships between groundwater and NPP/SOC across multiple ecosystems globally, though the conclusions drawn are necessarily limited by the quality of the input datasets. Spatial patterns of WTD-NPP and WTD-SOC correlations we documented could help guide groundwater management and policy development in different regions (Cord *et al* 2017). For example, in regions where positive WTD-NPP and WTD-SOC correlations were concentrated (e.g., central North America), with high temperature and dry conditions, long-term attention should be paid to the sustainable use and extraction of groundwater (Gleeson *et al* 2010). Drawdown of the water table in these regions can lead to unexpected cascading effects on multiple ES beyond freshwater supply, for example, NPP and SOC as revealed in this study, along with streamflow depletion (Zipper *et al* 2021, 2022b) and a loss of stream species (Stubbington *et al* 2020). In contrast, for basins in South Asia, where negative WTD-NPP and WTD-SOC relationships were predominant, measures, such as drainage or alternate irrigation during land management to lower WTD may have benefits (Sarker *et al* 2020), though drainage could also be associated with ecosystem disservices such as impaired surface water quality (Gramlich *et al* 2018, Nazari *et al* 2021). Due to the bias of WTD, NPP and SOC observational data towards temperate latitudes in North America and Europe, the implications and mechanisms of these WTD-NPP/SOC correlations may be more robust for these geographic regions.

Our finding that WTD-NPP and WTD-SOC correlations varied in response to climate factors will provide insights for understanding potential changes of groundwater effects under future climate change (e.g., warming and more frequent extreme events, such as drought). Among climatic factors, temperature emerged as the most important driver mediating groundwater correlations with both NPP and SOC, indicating that regions more susceptible to future global warming would experience the most drastic changes in the influences of groundwater. For example, in regions with projected temperature increases, the importance of groundwater on sustaining NPP or SOC will also be likely to increase, but, ironically, these regions may at the same time experience lower groundwater levels from reduced groundwater recharge and increased irrigation requirements (Green *et al* 2011, Crosbie *et al* 2013, Rodell *et al* 2018). Previous work has found that severe droughts caused multi-year declines in terrestrial NPP and could further degrade terrestrial carbon pools (Zhao and Running 2010), but subsidies from sustained groundwater levels may effectively moderate this scenario (Vicente-Serrano *et al* 2020). In addition, substantial spatial variations in groundwater effects and their response to climate factors highlight that groundwater effects tend not to be static and thus a more dynamic approach to understanding and managing groundwater to enhance the sustainable provision of ES may be required (Elshall *et al* 2020).

Our research has some limitations. Due to data availability, only groundwater effects on NPP and SOC were considered in our analysis; thus, groundwater effects on a broad array of other ES still require future investigations. Past local- to regional-scale

work has demonstrated that changes in WTD can interact with SOC to further influence crop yield and biogeochemical cycling (Pohl *et al* 2015, Huang *et al* 2021). Hence, groundwater influences on synergies or tradeoffs among multiple ES needs to be further explored. Additionally, we used static, global WTD and SOC products derived from observational data that are not uniformly distributed (Zhao *et al* 2005, Fan *et al* 2013, Hengl *et al* 2017) and were therefore unable to identify how NPP and SOC respond to interannual or seasonal groundwater level changes that can be caused by natural fluctuations or artificial disturbances. These interannual WTD changes and effects could be a major concern for water use policy or groundwater management (Tiemeyer *et al* 2016), and merit future investigation (e.g., using coupled dynamic large-scale groundwater–ecosystem models or future datasets with improved spatial and temporal resolutions). The development of such interdisciplinary research on the dynamics of groundwater and its social-ecological effects is necessary in the context of environmental change and socioeconomic development.

## 5. Conclusion

Our work revealed that groundwater effects on NPP and SOC were spatially heterogeneous and differed depending on the type of ES across the globe. We identified multiple environmental factors that mediated groundwater relationships with two ES indicators, particularly for climate (temperature, precipitation and aridity) and land use (vegetation extent) factors. Constraint effects on WTD-NPP/SOC correlations imply that climate changes may saturate potential groundwater relationships with NPP and SOC. In tandem, our work suggests that future ES research should address potential conservation and holistic management implications of changes to groundwater flows and levels. The widespread WTD-NPP and WTD-SOC relationships we detected indicate that climate and land-use changes that alter groundwater dynamics may have cascading impacts on the sustainable provision of ES through different biogeochemical and hydrological pathways. Our study highlights the importance of integrating multiple sources and disparate datasets to understand large-scale ES patterns and dynamics, their environmental controls and responses to current and future environmental changes.

## Data availability statement

All data that support the findings of this study are included within the article (and any supplementary files). The R code and data for statistical analysis can be downloaded in: https://doi.org/10.6084/m9.figshare.23694354.

## Acknowledgments

Funding support of this work comes from USDA National Institute of Food and Agriculture, Hatch (FLA-FTL-005640), McIntire-Stennis (FLA-FTL-005673) and AFRI Foundational and Applied Science Program (GRANT13070634) Projects. This research was also partially supported by Guangdong Basic and Applied Basic Research Foundation (2020A1515011265), Value Realization of Nature Conservation Areas Foundation (Forestry Administration of Guangdong Province), Guangdong Provincial Construction Project of Agricultural Science and Technology Innovation and Extension System (2023KJ360), Hongda Zhang Scientific Research Fund, Sun Yat-Sen University and Chinese Scholarship Council.

## ORCID iDs

Bei Huang https://orcid.org/0000-0002-7482-3267
Sam Zipper https://orcid.org/0000-0002-8735-5757
Shaolin Peng https://orcid.org/0000-0001-7033-8929
Jiangxiao Qiu https://orcid.org/0000-0002-3741-5213

## References

Aeschbach-Hertig W and Gleeson T 2012 Regional strategies for the accelerating global problem of groundwater depletion *Nat. Geosci.* **5** 853–61

Bangroo S A, Najar G R, Achin E and Truong P N 2020 Application of predictor variables in spatial quantification of soil organic carbon and total nitrogen using regression kriging in the North Kashmir forest Himalayas *Catena* **193** 104632

Bartholomé E and Belward A S 2005 GLC2000: a new approach to global land cover mapping from Earth observation data *Int. J. Remote Sens.* **26** 1959–77

Barton K 2009 MuMIn: multi-model inference (available at: http://r-forge.r-project.org/projects/mumin/)

Bivand R 2022 R packages for analyzing spatial data: a comparative case study with areal data *Geogr. Anal.* **54** 488–518

Borrelli P *et al* 2017 An assessment of the global impact of 21st century land use change on soil erosion *Nat. Commun.* **8** 2013

Burnham K P and Anderson D R 2004 Multimodel inference: understanding AIC and BIC in model selection *Sociol. Methods Res.* **33** 261–304

Cade B S and Noon B R 2003 A gentle introduction to quantile regression for ecologists *Front. Ecol. Environ.* **1** 412–20

Callesen I, Liski J, Raulund-Rasmussen K, Olsson M T, Tau-Strand L, Vesterdal L and Westman C J 2003 Soil carbon stores in Nordic well-drained forest soils—relationships with climate and texture class *Glob. Change Biol.* **9** 358–70

Chapin F S, Matson P A and Vitousek P M 2011 Carbon inputs to ecosystems *Principles of Terrestrial Ecosystem Ecology* ed F S Chapin, P A Matson and P M Vitousek (Springer) pp 123–56

Chen G, Bai J, Wang J, Liu Z and Cui B 2022 Responses of soil respiration to simulated groundwater table and salinity fluctuations in tidal freshwater, brackish and salt marshes *J. Hydrol.* **612** 128215

Churkina G, Running S W and Schloss A L (The Participants of the Potsdam NPP Model Intercomparison) 1999 Comparing global models of terrestrial net primary productivity (NPP): the importance of water availability *Glob. Change Biol.* **5** 46–55

Ciruzzi D M and Loheide S P II 2021 Groundwater subsidizes tree growth and transpiration in sandy humid forests *Ecohydrology* **14** e2294

Collalti A and Prentice I C 2019 Is NPP proportional to GPP? Waring's hypothesis 20 years on *Tree Physiol.* **39** 1473–83

Cord A F, Brauman K A, Chaplin-Kramer R, Huth A, Ziv G and Seppelt R 2017 Priorities to advance monitoring of ecosystem services using earth observation *Trends Ecol. Evol.* **32** 416–28

Crosbie R S, Scanlon B R, Mpelasoka F S, Reedy R C, Gates J B and Zhang L 2013 Potential climate change effects on groundwater recharge in the high plains aquifer, USA *Water Resour. Res.* **49** 3936–51

Cuthbert M O, Gleeson T, Moosdorf N, Befus K M, Schneider A, Hartmann J and Lehner B 2019 Global patterns and dynamics of climate–groundwater interactions *Nat. Clim. Change* **9** 137–41

Danielopol D L, Pospisil P and Rouch R 2000 Biodiversity in groundwater: a large-scale view *Trends Ecol. Evol.* **15** 223–4

de Graaf I E M, Gleeson T, van Beek L P H, Sutanudjaja E H and Bierkens M F P 2019 Environmental flow limits to global groundwater pumping *Nature* **574** 90–94

Deng L, Liu G and Shangguan Z 2014 Land-use conversion and changing soil carbon stocks in China's 'Grain-for-Green' program: a synthesis *Glob. Change Biol.* **20** 3544–56

Elshall A S, Arik A D, El-Kadi A I, Pierce S, Ye M, Burnett K M, Wada C A, Bremer L L and Chun G 2020 Groundwater sustainability: a review of the interactions between science and policy *Environ. Res. Lett.* **15** 093004

Fan Y 2015 Groundwater in the Earth's critical zone: relevance to large-scale patterns and processes *Water Resour. Res.* **51** 3052–69

Fan Y, Li H and Miguez-Macho G 2013 Global patterns of groundwater table depth *Science* **339** 940–3

Fan Y, Miguez-Macho G, Jobbágy E G, Jackson R B and Otero-Casal C 2017 Hydrologic regulation of plant rooting depth *Proc. Natl Acad. Sci.* **114** 10572–7

Gleeson T, Cuthbert M, Ferguson G and Perrone D 2020 Global groundwater sustainability, resources, and systems in the anthropocene *Annu. Rev. Earth Planet. Sci.* **48** 431–63

Gleeson T, VanderSteen J, Sophocleous M A, Taniguchi M, Alley W M, Allen D M and Zhou Y 2010 Groundwater sustainability strategies *Nat. Geosci.* **3** 378–9

Gramlich A, Stoll S, Stamm C, Walter T and Prasuhn V 2018 Effects of artificial land drainage on hydrology, nutrient and pesticide fluxes from agricultural fields—a review *Agric. Ecosyst. Environ.* **266** 84–99

Green J K, Seneviratne S I, Berg A M, Findell K L, Hagemann S, Lawrence D M and Gentine P 2019 Large influence of soil moisture on long-term terrestrial carbon uptake *Nature* **565** 476–9

Green T R, Taniguchi M, Kooi H, Gurdak J J, Allen D M, Hiscock K M, Treidel H and Aureli A 2011 Beneath the surface of global change: impacts of climate change on groundwater *J. Hydrol.* **405** 532–60

Guan Y, Bai J, Wang J, Wang W, Wang X, Zhang L, Li X and Liu X 2021 Effects of groundwater tables and salinity levels on soil organic carbon and total nitrogen accumulation in coastal wetlands with different plant cover types in a Chinese estuary *Ecol. Indic.* **121** 106969

Hare D K, Helton A M, Johnson Z C, Lane J W and Briggs M A 2021 Continental-scale analysis of shallow and deep groundwater contributions to streams *Nat. Commun.* **12** 1450

Hengl T *et al* 2014 SoilGrids1km—Global soil information based on automated mapping *PLoS One* **9** e105992

Hengl T *et al* 2017 SoilGrids250m: global gridded soil information based on machine learning *PLoS One* **12** e0169748

Hijmans R J, Cameron S E, Parra J L, Jones P G and Jarvis A 2005 Very high resolution interpolated climate surfaces for global land areas *Int. J. Climatol.* **25** 1965–78

Huang J, Hartemink A E and Kucharik C J 2021 Soil-dependent responses of US crop yields to climate variability and depth to groundwater *Agric. Syst.* **190** 103085

Jobbágy E G and Jackson R B 2000 The vertical distribution of soil organic carbon and its relation to climate and vegetation *Ecol. Appl.* **10** 423–36

Jobbágy E G, Nosetto M D, Villagra P E and Jackson R B 2011 Water subsidies from mountains to deserts: their role in sustaining groundwater-fed oases in a sandy landscape *Ecol. Appl.* **21** 678–94

Koirala S *et al* 2017 Global distribution of groundwater-vegetation spatial covariation *Geophys. Res. Lett.* **44** 4134–42

Linke S *et al* 2019 Global hydro-environmental sub-basin and river reach characteristics at high spatial resolution *Sci. Data* **6** 283

Liu L, Gudmundsson L, Hauser M, Qin D, Li S and Seneviratne S I 2020 Soil moisture dominates dryness stress on ecosystem production globally *Nat. Commun.* **11** 4892

Liu L and Wu J 2021 Ecosystem services-human wellbeing relationships vary with spatial scales and indicators: the case of China *Resour. Conserv. Recycl.* **172** 105662

Lowry C S and Loheide S P II 2010 Groundwater-dependent vegetation: quantifying the groundwater subsidy *Water Resour. Res.* **46** W06202

Lyon S W, Grabs T, Laudon H, Bishop K H and Seibert J 2011 Variability of groundwater levels and total organic carbon in the riparian zone of a boreal catchment *J. Geophys. Res. Biogeosci.* **116** G01020

Maxwell R M and Condon L E 2016 Connections between groundwater flow and transpiration partitioning *Science* **353** 377–80

Meersmans J, Van Wesemael B, Goidts E, Van MOLLE M, De Baets S and De Ridder F 2011 Spatial analysis of soil organic carbon evolution in Belgian croplands and grasslands, 1960–2006 *Glob. Change Biol.* **17** 466–79

Miguez-Macho G and Fan Y 2021 Spatiotemporal origin of soil water taken up by vegetation *Nature* **598** 624–8

Mills A J, Fey M V, Gröngröft A, Petersen A and Medinski T V 2006 Unravelling the effects of soil properties on water infiltration: segmented quantile regression on a large data set from arid south-west Africa *Soil Res.* **44** 783–97

Mitchell M G E, Bennett E M and Gonzalez A 2014 Forest fragments modulate the provision of multiple ecosystem services *J. Appl. Ecol.* **51** 909–18

Nazari S, Ford W I and King K W 2021 Quantifying hydrologic pathway and source connectivity dynamics in tile drainage: implications for phosphorus concentrations *Vadose Zone J.* **20** e20154

Orellana F, Verma P, Loheide S P II and Daly E 2012 Monitoring and modeling water-vegetation interactions in groundwater-dependent ecosystems *Rev. Geophys.* **50** RG3003

Pesaresi M and Freire S 2016 GHS-SMOD R2016A—GHS settlement grid, following the REGIO model 2014 in application to GHSL Landsat and CIESIN GPW v4-multitemporal (1975–1990-2000-2015)—OBSOLETE RELEASE (European Commission, Joint Research Centre (JRC))

Poeplau C, Jacobs A, Don A, Vos C, Schneider F, Wittnebel M, Tiemeyer B, Heidkamp A, Prietz R and Flessa H 2020 Stocks of organic carbon in German agricultural soils—Key results of the first comprehensive inventory *J. Plant Nutr. Soil Sci.* **183** 665–81

Pohl M, Hoffmann M, Hagemann U, Giebels M, Albiac Borraz E, Sommer M and Augustin J 2015 Dynamic C and N

stocks—key factors controlling the C gas exchange of maize in heterogenous peatland *Biogeosciences* **12** 2737–52
Porada P, Van Stan J T and Kleidon A 2018 Significant contribution of non-vascular vegetation to global rainfall interception *Nat. Geosci.* **11** 563–7
Prananto J A, Minasny B, Comeau L-P, Rudiyanto R and Grace P 2020 Drainage increases $CO_2$ and $N_2O$ emissions from tropical peat soils *Glob. Change Biol.* **26** 4583–600
Qiao J, Yu D, Cao Q and Hao R 2019 Identifying the relationships and drivers of agro-ecosystem services using a constraint line approach in the agro-pastoral transitional zone of China *Ecol. Indic.* **106** 105439
Qiu J, Zipper S C, Motew M, Booth E G, Kucharik C J and Loheide S P 2019 Nonlinear groundwater influence on biophysical indicators of ecosystem services *Nat. Sustain.* **2** 475–83
R Core Team 2022 R: a language and environment for statistical computing (available at: www.R-project.org/)
Rizzo G, Edreira J I R, Archontoulis S V, Yang H S and Grassini P 2018 Do shallow water tables contribute to high and stable maize yields in the US Corn Belt? *Glob. Food Secur.* **18** 27–34
Robinson N, Regetz J and Guralnick R P 2014 EarthEnv-DEM90: a nearly-global, void-free, multi-scale smoothed, 90m digital elevation model from fused ASTER and SRTM data *ISPRS J. Photogramm. Remote Sens.* **87** 57–67
Rodell M, Famiglietti J S, Wiese D N, Reager J T, Beaudoing H K, Landerer F W and Lo M-H 2018 Emerging trends in global freshwater availability *Nature* **557** 651–9
Sarker K K, Hossain A, Timsina J, Biswas S K, Malone S L, Alam M K, Loescher H W and Bazzaz M 2020 Alternate furrow irrigation can maintain grain yield and nutrient content, and increase crop water productivity in dry season maize in sub-tropical climate of South Asia *Agric. Water Manage.* **238** 106229
Siebert S, Burke J, Faures J M, Frenken K, Hoogeveen J, Döll P and Portmann F T 2010 Groundwater use for irrigation—a global inventory *Hydrol. Earth Syst. Sci.* **14** 1863–80
Siebert S, Kummu M, Porkka M, Döll P, Ramankutty N and Scanlon B R 2015 A global data set of the extent of irrigated land from 1900 to 2005 *Hydrol. Earth Syst. Sci.* **19** 1521–45
Soylu M E, Kucharik C J and Loheide S P 2014 Influence of groundwater on plant water use and productivity: development of an integrated ecosystem—variably saturated soil water flow model *Agric. For. Meteorol.* **189–190** 198–210
Staal A, Tuinenburg O A, Bosmans J H C, Holmgren M, van Nes E H, Scheffer M, Zemp D C and Dekker S C 2018 Forest-rainfall cascades buffer against drought across the Amazon *Nat. Clim. Change* **8** 539–43
Stubbington R, Acreman M, Acuña V, Boon P J, Boulton A J, England J, Gilvear D, Sykes T and Wood P J 2020 Ecosystem services of temporary streams differ between wet and dry phases in regions with contrasting climates and economies *People Nat.* **2** 660–77
Tiemeyer B *et al* 2016 High emissions of greenhouse gases from grasslands on peat and other organic soils *Glob. Change Biol.* **22** 4134–49
Turetsky M R *et al* 2014 A synthesis of methane emissions from 71 northern, temperate, and subtropical wetlands *Glob. Change Biol.* **20** 2183–97
Vicente-Serrano S M, Quiring S M, Peña-Gallardo M, Yuan S and Domínguez-Castro F 2020 A review of environmental droughts: increased risk under global warming? *Earth Sci. Rev* **201** 102953
Wada Y, van Beek L P H and Bierkens M F P 2012 Nonsustainable groundwater sustaining irrigation: a global assessment *Water Resour. Res.* **48** W00L06
Wen Y, Freeman B, Ma Q, Evans C D, Chadwick D R, Zang H and Jones D L 2020 Raising the groundwater table in the non-growing season can reduce greenhouse gas emissions and maintain crop productivity in cultivated fen peats *J. Clean. Prod.* **262** 121179
Wu Z, Dijkstra P, Koch G W, Peñuelas J and Hungate B A 2011 Responses of terrestrial ecosystems to temperature and precipitation change: a meta-analysis of experimental manipulation *Glob. Change Biol.* **17** 927–42
Zhang Y, Xu M, Chen H and Adams J 2009 Global pattern of NPP to GPP ratio derived from MODIS data: effects of ecosystem type, geographical location and climate *Glob. Ecol. Biogeogr.* **18** 280–90
Zhao M, Heinsch F A, Nemani R R and Running S W 2005 Improvements of the MODIS terrestrial gross and net primary production global data set *Remote Sens. Environ.* **95** 164–76
Zhao M and Running S W 2010 Drought-induced reduction in global terrestrial net primary production from 2000 through 2009 *Science* **329** 940–3
Zipper S C *et al* 2021 Pervasive changes in stream intermittency across the United States *Environ. Res. Lett.* **16** 084033
Zipper S C, Farmer W H, Brookfield A, Ajami H, Reeves H W, Wardropper C, Hammond J C, Gleeson T and Deines J M 2022a Quantifying streamflow depletion from groundwater pumping: a practical review of past and emerging approaches for water management *JAWRA J. Am. Water Resour. Assoc.* **58** 289–312
Zipper S C, Soylu M E, Booth E G and Loheide S P II 2015 Untangling the effects of shallow groundwater and soil texture as drivers of subfield-scale yield variability *Water Resour. Res.* **51** 6338–58
Zipper S C, Soylu M E, Kucharik C J and Loheide S P II 2017 Quantifying indirect groundwater-mediated effects of urbanization on agroecosystem productivity using MODFLOW-AgroIBIS (MAGI), a complete critical zone model *Ecol. Modelling* **359** 201–19
Zipper S, Popescu I, Compare K, Zhang C and Seybold E C 2022b Alternative stable states and hydrological regime shifts in a large intermittent river *Environ. Res. Lett.* **17** 074005
Zomer R J, Trabucco A, Bossio D A and Verchot L V 2008 Climate change mitigation: a spatial analysis of global land suitability for clean development mechanism afforestation and reforestation *Agric. Ecosyst. Environ.* **126** 67–80